# Quantification and Analyses of $N_2O$ Emission and Testing of Relevant $N_2O$ Control Technology at Avedøre Wastewater Treatment Plant

- Served as the technical report for VUDP project "Demonstration af en ny kontrol metode til at reducere lattergas udledningen fra renseanlæg" (ID No. 87.2016)
- Prepared by Xueming Chen and Gürkan Sin, Process and Systems Engineering Center (PROSYS), Department of Chemical and Biochemical Engineering, Technical University of Denmark

# 1. PROJECT DESCRIPTION

## 1.1. Background

The production and emission of nitrous oxide ($N_2O$), a potent greenhouse gas (GHG) with a global warming effect 265 times stronger than carbon dioxide on a 100-year time horizon [1], significantly increase the carbon footprint of wastewater treatment plants (WWTPs) and therefore contribute substantially to the global GHG stock [2, 3]. To further anchor the leading position of Denmark in the water sector, Danish WWTPs will soon be obliged to report their carbon footprint and resort to technological solutions to control $N_2O$ emission.

Despite the fixed, low level of 0.035% suggested by IPCC based on some foreign WWTPs [1], a significantly varied full-scale $N_2O$ emission factor has been reported, ranging from 0 to 14.6% relative to incoming nitrogen [3-7]. This variability is due to the existence of multiple $N_2O$ production contributing pathways (including nitrifier denitrification pathway and hydroxylamine pathway by ammonium-oxidizing bacteria (AOB) as well as heterotrophic denitrification pathway by heterotrophic bacteria (HB)), which are mediated by a group of functional microorganisms and regulated by a number of affecting process variables. Long-term measurement campaigns, which are rarely reported, are therefore needed to clearly demonstrate full-scale $N_2O$ emission characteristics as well as to reliably deduce the

relationships between $N_2O$ emission and relevant process variables, serving as the basis for developing viable $N_2O$ control strategies.

With respect to $N_2O$ control strategies, only limited work based on model simulations has been reported. For example, the research team at Technical University of Denmark (DTU) reported a fuzzy logic controller targeted at controlling full-scale $N_2O$ emission using simulation models[8]. However, full-scale testing is still needed to verify the effectiveness of the reported controller. In fact, that the numerous $N_2O$ models available are seldom calibrated or verified using highly dynamic full-scale data in the long term already brings high uncertainty to the validity of the model-based $N_2O$ control strategies. In this case, data-driven development of $N_2O$ control strategies, which is rarely performed, is used as a reliable alternative.

## 1.2. Objectives

This project is based on a full-scale Danish WWTP (Avedøre WWTP operated by BIOFOS A/S) with plant design and control scheme commonly adopted by European WWTPs and aims to obtain full-scale $N_2O$ emission magnitude and characteristics for a better understanding of the control problem. The analysis results will be used to assess the applicability of the fuzzy logic controller developed by the DTU research team [8]. If the assumption/theory of the fuzzy logic controller is not well supported or its full-scale implementation is hard to achieve, improvements to the underlying concept of the fuzzy logic controller will be explored or alternative new ideas will be proposed based on the analysis results. Through incorporating the alternative controller into the existing monitoring/control system and making use of the hardware already available, an integrated solution capable of mitigating $N_2O$ emission will be formulated, the effectiveness of which will be tested at Avedøre WWTP.

# 2. METHODOLOGY

## 2.1. Plant/Process Description

With a capacity of serving approximately 350,000 PE, Avedøre WWTP treats around 70,000 $m^3$ of wastewater daily under dry weather conditions. Combined with screening, grit removal, primary settlement, and secondary clarification in the mainstream treatment, activated sludge process is applied in four Carrousel reactors working in parallel, each consisting of two

compartments alternatively fed and intermittently aerated as aerobic (aerated) or anoxic (non-aerated) zones (**Fig. 1**). Aeration is achieved with bubble diffusers mounted at the bottom of compartments and is activated when dissolved oxygen (DO) concentration is lower than the DO set-point which is determined based on in-situ $NH_4^+$ concentration and is pre-set in the STAR Control® implemented. The STAR Control® also regulates the entering/exiting of aerobic/anoxic phase of each compartment through the pre-set relationship between in-situ $NH_4^+$ and $NO_3^-$ concentrations, thus ensuring good nitrogen removal performance. For the side-stream treatment, anaerobic digestion is applied to produce biogas from primary and secondary sludge, which is then harvested for electricity generation.
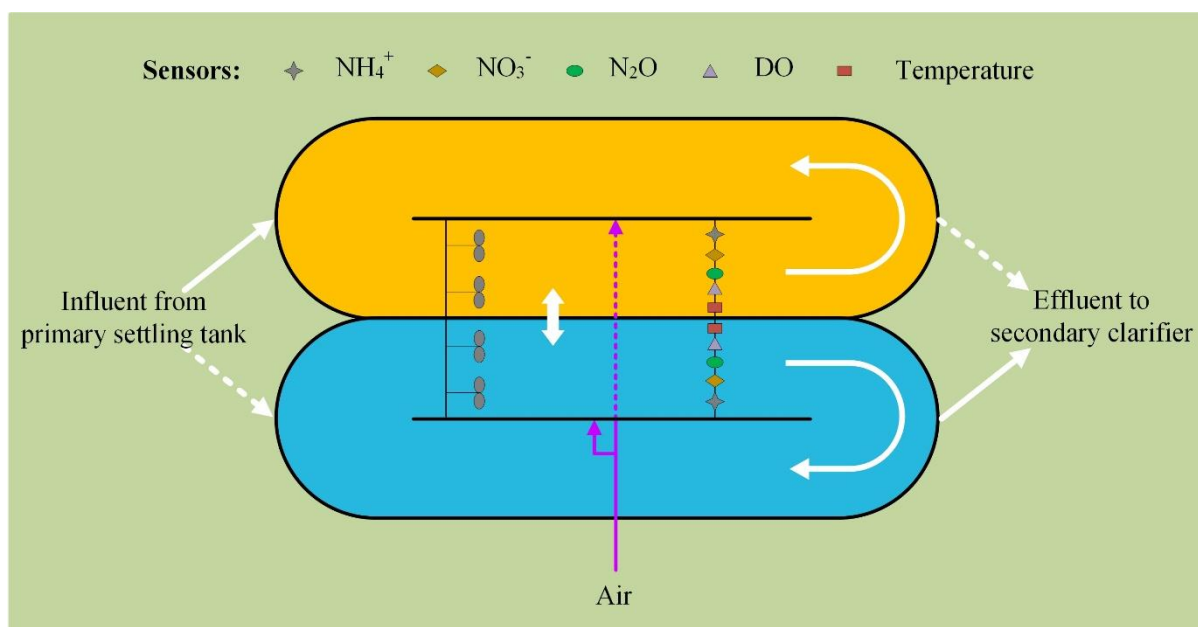


**Figure 1**. Schematic diagram of Carrousel reactor comprising two alternatively fed and intermittently aerated compartments at Avedøre WWTP (Locations of measuring sensors with respect to water flow direction are marked).

$NH_4^+$-N, $NO_3^-$-N, DO, and water temperature are constantly monitored in both compartments of all four reactors, while liquid-phase $N_2O$ is additionally measured using Unisense® sensors in two reactors (i.e., Reactor 1 and Reactor 3). As indicated in **Fig. 1**, the measuring sensors are placed in the same location with respect to the water flow direction in each compartment. All sensors are frequently calibrated and tested, thus ensuring the accuracy of measurements. Instead of the direct measurement of airflow rate into each compartment, the

opening of aeration valve in each compartment and the total airflow into all reactors are monitored. Influent flowrate into each reactor is also recorded online using a flow meter. Composite samples over 24 h are analyzed every one or two weeks to indicate influent quality.

## 2.2. Analyses on N₂O Emission

### 2.2.1. Data processing

After being extracted from the supervisory control and data acquisition (SCADA) system, the data during the 12-month monitoring period spanning **from March 2018 to February 2019** was firstly processed to ensure its quality through i) data synchronization under the same time-stamp and ii) removal of unreliable measurements (e.g., significantly negative readings due to sensor drifting, readings outside the sensor measurement range, and readings taken when sensors were not in service). The on-line data for all process variables investigated was aggregated into averages every 5 minutes for subsequent analyses and interpretations.

### 2.2.2. N₂O emission rate calculation

To calculate N₂O emission rate, equations were differentiated for aerobic (aerated) and anoxic (non-aerated) zones as follows [9]:

Aerobic (aerated) zone: $r_{N2O} = H_{N2O} \times S_{N2O} \times \left[ 1 - e^{-\frac{K_L a_{N2O}^{Aerated}}{H_{N2O}} \frac{V_R}{Q_A}} \right] \times \frac{Q_A}{V_R}$ (1)

Anoxic (non-aerated) zone: $r_{N2O} = K_L a_{N2O}^{Non-aerated} \times \left[ S_{N2O} - \frac{C_{N2O,air}}{H_{N2O}} \right]$ (2)

$r_{N2O}$: Volumetric N₂O emission rate (g-N m⁻³ d⁻¹), $H_{N2O}$: Dimensionless Henry's constant, $S_{N2O}$: Liquid-phase N₂O concentration (g-N m⁻³), $K_L a_{N2O}^{Aerated}$: Aerated N₂O mass transfer coefficient (d⁻¹), $V_R$: Volume of aerated part (m³), $Q_A$: Airflow rate (m³ d⁻¹), $K_L a_{N2O}^{Non-aerated}$: Non-aerated N₂O mass transfer coefficient (d⁻¹), $C_{N2O,air}$: N₂O concentration in air equilibrium (g-N m⁻³).

$K_L a_{N2O}^{Aerated}$ was determined according to Eq. 3 [10], while $K_L a_{N2O}^{Non-aerated}$ was calculated following Eq. 4 [11].

$$K_L a_{N2O}^{Aerated} = \left[\frac{D_R}{0.815}\right]^{-0.49} \times 34500 \times \left[\frac{Q_A}{S_A}\right]^{0.86} \times 1.024^{(T-20)} \tag{3}$$

$$K_L a_{N2O}^{Non-aerated} = 2 \times 1.024^{(T-20)} \tag{4}$$

$D_R$: Depth over diffusers (m), $S_A$: Size of aeration field (m$^2$), T: Temperature (°C).

### 2.2.3. Pearson's partial correlation analysis

A clear understanding of the impacts of process variables on N$_2$O emission is the key to the reliable formulation of N$_2$O control strategies. To this end, Pearson's partial correlation which measures the degree of association between two variables with the effect of other affecting variables removed was used. Using N$_2$O emission rate as the outcome variable and relevant process variables (NH$_4^+$-N, NO$_3^-$-N, DO, water temperature, influent, etc.) as the affecting variables, Pearson's partial correlation analysis, which accounted for the contributions of other affecting variables while indicating the individual contribution of the process variable studied to N$_2$O emission, returned a coefficient (PCC) in the range from -1 to 1. The value -1 (1) conveyed a perfect negative (positive) linear relationship between N$_2$O emission rate and the affecting variable investigated, while the value 0 indicated that there was no linear relationship. Pearson's partial correlation analysis was conducted using a MATLAB function in Statistics and Machine Learning Toolbox called partialcorri, which also returned a p-value for testing the hypothesis of no partial correlation against the alternative that there was a non-zero partial correlation. If the p-value was less than 0.05, then the partial correlation was regarded as significantly different from zero, thus confirming the important role of the relevant process variable in affecting/contributing to N$_2$O emission.

## 2.3. N$_2$O Control Technology and Relevant Testing

The fuzzy logic controller developed by the DTU research team [8] is based on the assumption that an effective minimization of N$_2$O emission could be achieved by slowing down the nitrifier denitrification pathway by AOB. To this end, complete nitrification should be pursued. In other words, the ammonium oxidized by AOB in the aerobic zone should be converted into nitrate by nitrite-oxidizing bacteria (NOB) as much as possible so that the formation of nitrite as the

trigger for the nitrifier denitrification pathway could be minimized. Therefore, the ratio between overall nitrate nitrogen produced and overall ammonium nitrogen depleted in the aerobic zone ($R_{NatAmm}$), expressed in Eq. 5, is used as the controlled variable.

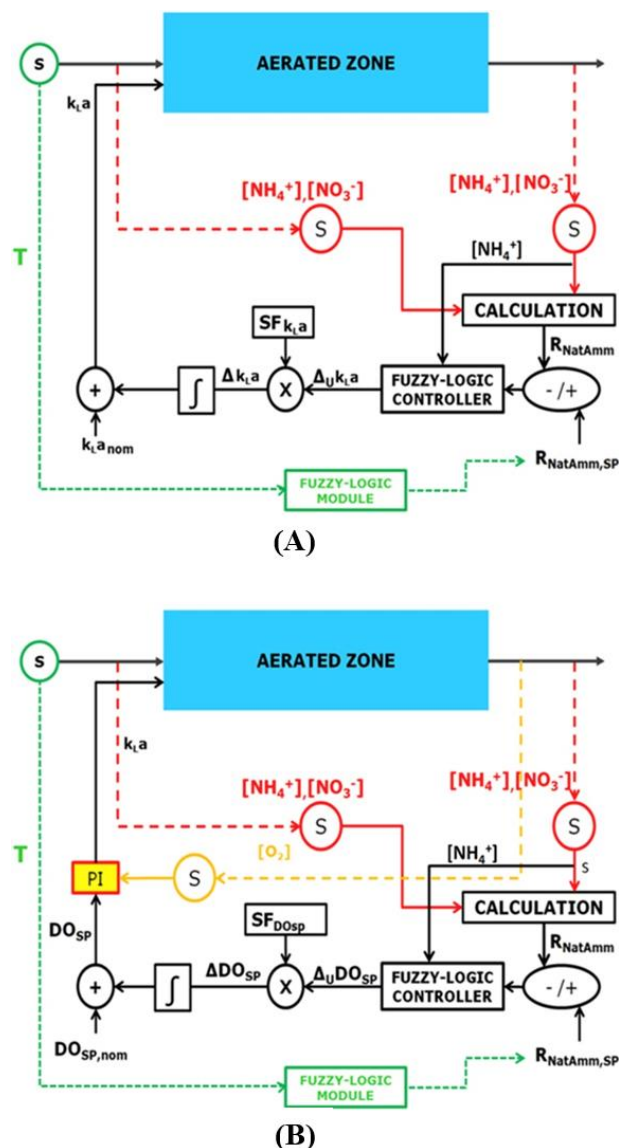$$R_{NatAmm} = \frac{NO_3^{-,out} - NO_3^{-,in}}{NH_4^{+,in} - NH_4^{+,out}} \tag{5}$$



**(A)**



**(B)**

**Figure 2**. Control system implementation using (**A**) oxygen mass transfer coefficient $k_La$ and (**B**) set-point of dissolved oxygen concentration $DO_{SP}$ as manipulated variable (adopted from Boiocchi et al.[8]).

Regarding the manipulated variable used to achieve the control objective, either the air supply (i.e., oxygen mass transfer coefficient $k_La$) or the DO set-point ($DO_{SP}$) of a Proportional Integral (PI) controller will be adopted to regulate the oxygen availability in the aerobic zone. Based on the selection of manipulated variables, two generic control structures could be implemented in an aerobic zone of a WWTP for the minimization of $N_2O$ emission, as shown in **Fig. 2**. As can be seen, the measured ammonium and nitrate nitrogen concentrations in the inlet and outlet of the aerated zone are used for the calculation of $R_{NatAmm}$. The influent temperature to the system is used to update the set-point for $R_{NatAmm}$ (i.e., $R_{NatAmm,SP}$) through a fuzzy-logic module. The difference between $R_{NatAmm,SP}$ and $R_{NatAmm}$ is given as input to the fuzzy-logic control, which infers the unitary variation for the manipulated variable. This quantity therefore forms an indicator of whether the manipulated variable has to be increased or decreased. To attribute a physical dimension to this quantity, a scaling factor (either $SF_{kLa}$ or $SF_{DOsp}$), of the same order of magnitude as the nominal value of the corresponding manipulated variable, is multiplied with this quantity. By summing up these unit variations in time, the variations $\Delta k_La$ or $\Delta DO_{SP}$ constitute the difference between the value of the actual manipulated variable and its corresponding nominal value. The exact setting of the manipulated variable is thus known by adding its corresponding nominal value.

Due to the native constraint of the STAR® control implemented at Avedøre WWTP, it is technically not possible to integrate it with the fuzzy logic controller, unless the whole plant gets decommissioned for setting up new control algorithms. After probing into the characteristics of the STAR® control applied (through analysis of the STAR® control system in the plant-wide model of Avedøre WWTP implemented in WEST® software), we decided to test the main component of the fuzzy logic controller which is the aeration regulation to balance the AOB and NOB activities manually. In other words, we have manually manipulated and tested the DO set-point at Avedøre WWTP, which is doable in the STAR® control system and should also regulate the activities of AOB and NOB as suggested by the fuzzy logic controller. To this end, the DO set-point in one of the reactors with the installation of $N_2O$ sensors (i.e., Reactor 1 and Reactor 3) was increased/decreased by 0.5 g-$O_2$ m$^{-3}$, while the DO set-point remained unchanged in the other reactor.

Based on the analyses on full-scale N$_2$O emission, alternative control strategies were also proposed, which could be incorporated into the existing monitoring/control system of Avedøre WWTP to formulate an integrated solution capable of mitigating N$_2$O emission, the effectiveness of which warrants future testing at Avedøre WWTP.

# 3. RESULTS AND DISCUSSION

## 3.1. Determination of Airflow

As indicated in **Section 2.2.2**, the calculation of N$_2$O emission rate in the aerobic (aerated) zone necessitates the quantification of airflow into each compartment (i.e., $Q_A$). However, at Avedøre WWTP, only the total airflow into all compartments and the opening of aeration valve in each compartment are measured. In this case, based on the inherent characteristic curve of aeration valve, 4 possible models to describe the installed relationship between valve opening and airflow rate were proposed (see **Fig. 3**).
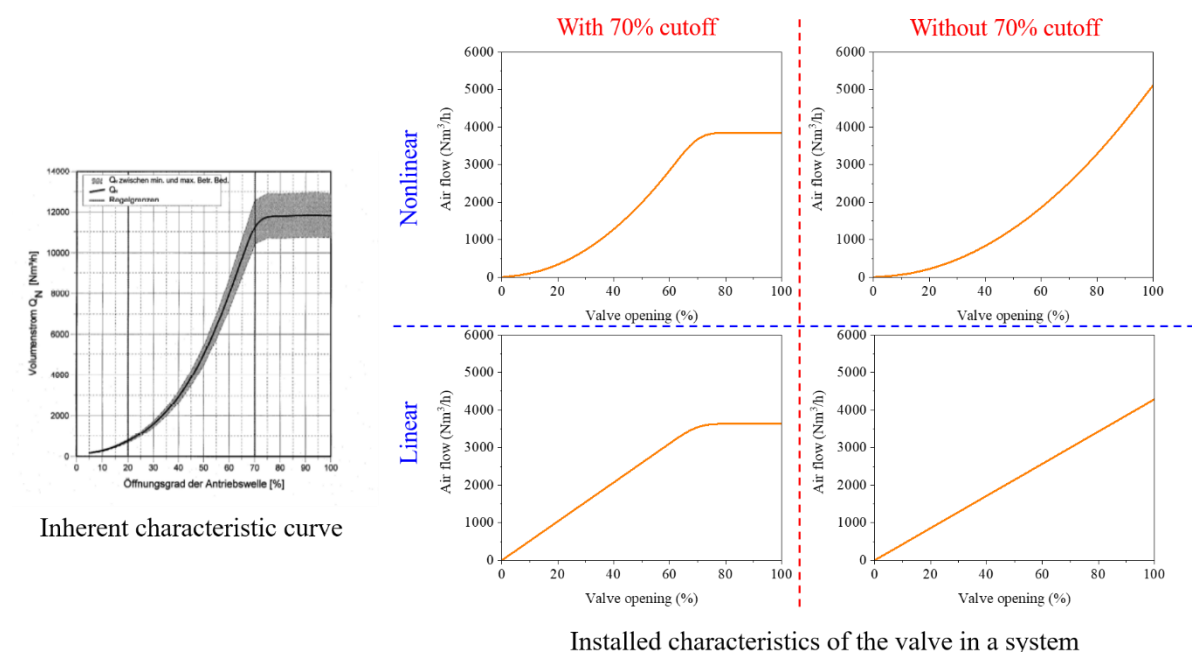


Inherent characteristic curve

Installed characteristics of the valve in a system

**Figure 3**. Inherent characteristic curve of aeration valve (x-axis: valve opening, y-axis: nominal airflow rate) and possible models to describe installed relationship between valve opening and airflow rate at Avedøre WWTP.
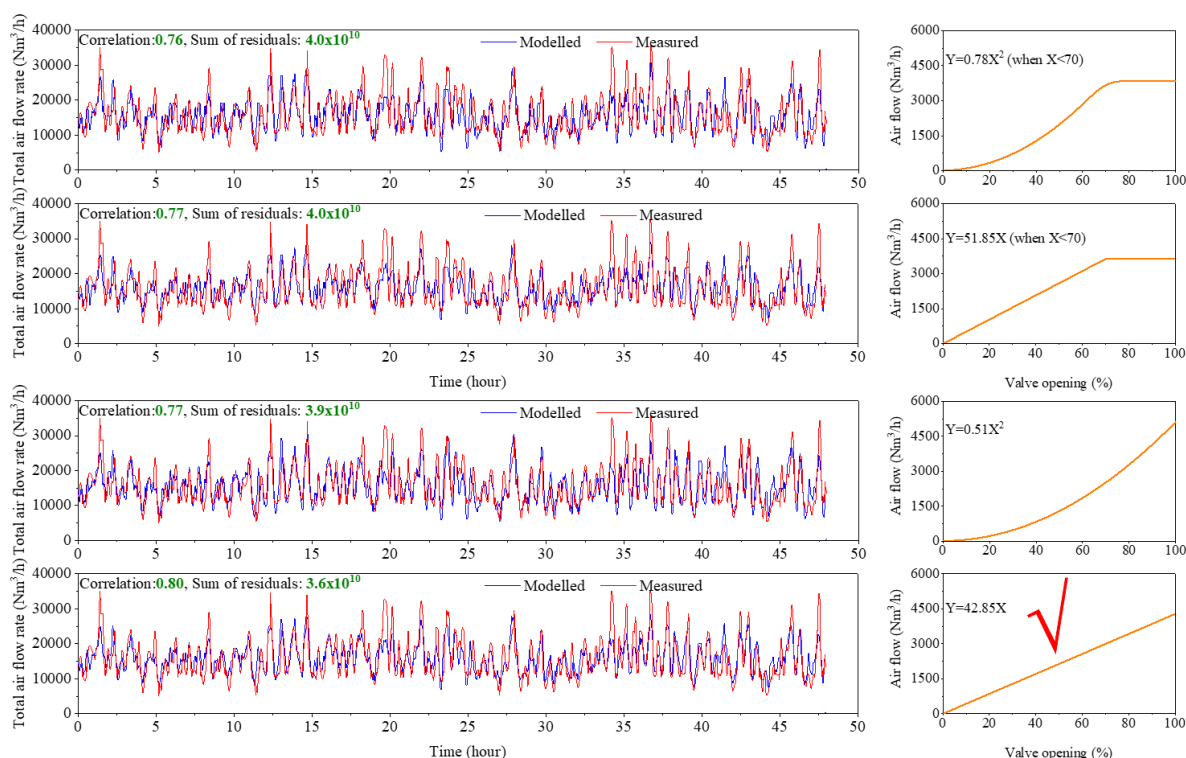
**Figure 4**. Comparison between modelled and measured total airflow rate.

Through comparing the modelled and measured total airflow rate (**Fig. 4**), the linear model without 70% cutoff was found to be the best option to estimate airflow based on valve opening and total airflow measurements as it generated the highest correlation ($R^2$) with the lowest sum of residuals. It is also noted that the other alternative models rendered a very close value of $R^2$, making them equally useful correlations. Therefore, $Q_A$ into each compartment was calculated by proportioning the total airflow measurement based on the ratio of the valve opening measurement in the compartment to the sum of all valve opening measurements.

## 3.1. Seasonal N₂O Emission at Avedøre WWTP

As depicted in **Fig. 5A**, a distinct relationship between monthly average of $N_2O$ emission rate and water temperature has been observed for Reactor 3 over the monitoring period. The average $N_2O$ emission rate was 0.77 g-N m$^{-3}$ d$^{-1}$ at the average water temperature of 10.7 °C in March 2018 when the monitoring campaign commenced. With the increasing water temperature, the

N$_2$O emission rate increased, reaching its peak monthly average of 2.30 g-N m$^{-3}$ d$^{-1}$ at the average water temperature of 16.4 °C in May 2018. Further increase in the water temperature brought down the N$_2$O emission rate, arriving at 0.45 g-N m$^{-3}$ d$^{-1}$ at the average water temperature of 20.6 °C in August 2018. Afterwards, the water temperature entered a decreasing stage. In September 2018 when the average water temperature was 19.8 °C, the minimum monthly average of N$_2$O emission rate was achieved at 0.01 g-N m$^{-3}$ d$^{-1}$. Continuous decrease in the water temperature towards 12.1 °C in February 2019 (i.e., the end of the monitoring campaign) led to the gradual recovery of the N$_2$O emission rate. With a high Pearson's correlation coefficient of 0.93 (p=0.00), the analogous results for Reactor 1 in **Fig. 5B** prove the reproducibility of the seasonal pattern of N$_2$O emission observed for Reactor 3 (i.e., **Fig. 5A**).

On the whole, the monitoring period could be divided into two sub-periods: sub-period with relatively high N$_2$O emission and sub-period with relatively low N$_2$O emission. As indicated in **Fig. 5**, the sub-period with relatively high N$_2$O emission was characterized by an increasing trend of water temperature (i.e., between March 2018 and August 2018), while the sub-period with relatively low N$_2$O emission was featured with a decreasing trend of water temperature (i.e., from August 2018 to February 2019). This dependency of N$_2$O emission on water temperature should be largely attributed to the various responses of functional microorganisms involved in nitrogen conversion reactions (including AOB, NOB, and HB) to changes in temperature. Although biological activities are known to accelerate with increasing temperature within a suitable temperature range, each type of functional microorganisms has its own specific temperature dependency, which could partially explain the fact that the maximum and minimum N$_2$O emission rates didn't correlate directly with the extremum water temperature conditions (see **Fig. 5A**). Moreover, the notably different magnitude of N$_2$O emission rates between the two parallel reactors operated under the same conditions in **Figs. 5A-B**, especially in the sub-period with relatively high N$_2$O emission, might also be the result of the different amount of biomass as well as the diverse local microbial community structures shaped after long-term operation. Therefore, monitoring on one reactor might not reflect the N$_2$O emission from other parallel reactors. In other words, reliable quantification of the plant-wide N$_2$O emission might necessitate respective monitoring on all different reactors. There is no doubt

that this argument would be further verified upon the future availability of additional $N_2O$ emission results of the other two parallel reactors.
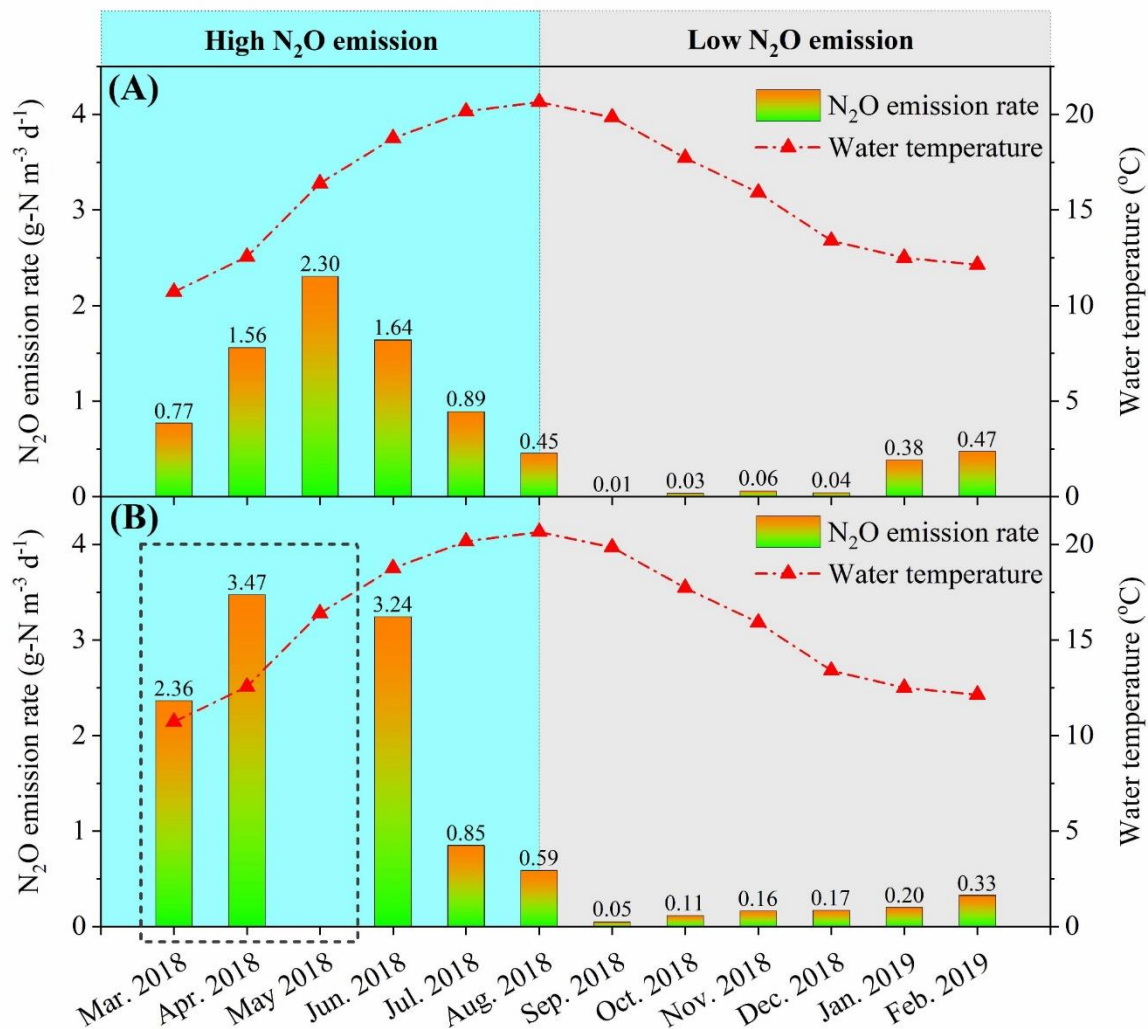


**Figure 5**. Seasonal $N_2O$ emission pattern in (**A**) Reactor 3 and (**B**) Reactor 1 (Highlighted box in (**B**) indicates months when $N_2O$ was only monitored in one compartment or both $N_2O$ sensors were not in service).

Using the off-line measured total Kjeldahl nitrogen (TKN) of composite samples to obtain the monthly average of nitrogen loading, the monthly $N_2O$ emission factor for Reactor 3 over the monitoring period was calculated to vary between 0.01% and 3.55%, with a yearly level of 1.05% (**Fig. 6**). These full-scale $N_2O$ emission factors resided well in the reported range from 0 to 14.6% organized by Daelman et al.[7] but were largely (11 out of 12 monitored months, i.e.,

except September 2018) higher than the level of 0.035% proposed by IPCC [1] (see **Fig. 6**). Therefore, guidelines provided by IPCC should be used with care in order to represent full-scale $N_2O$ emission. Considering the shortage of reliable modelling techniques capable of predicting long-term $N_2O$ emission as well as the rather complicated correlations between $N_2O$ emission and process variables, monitoring campaigns are still needed to report full-scale $N_2O$ emission.
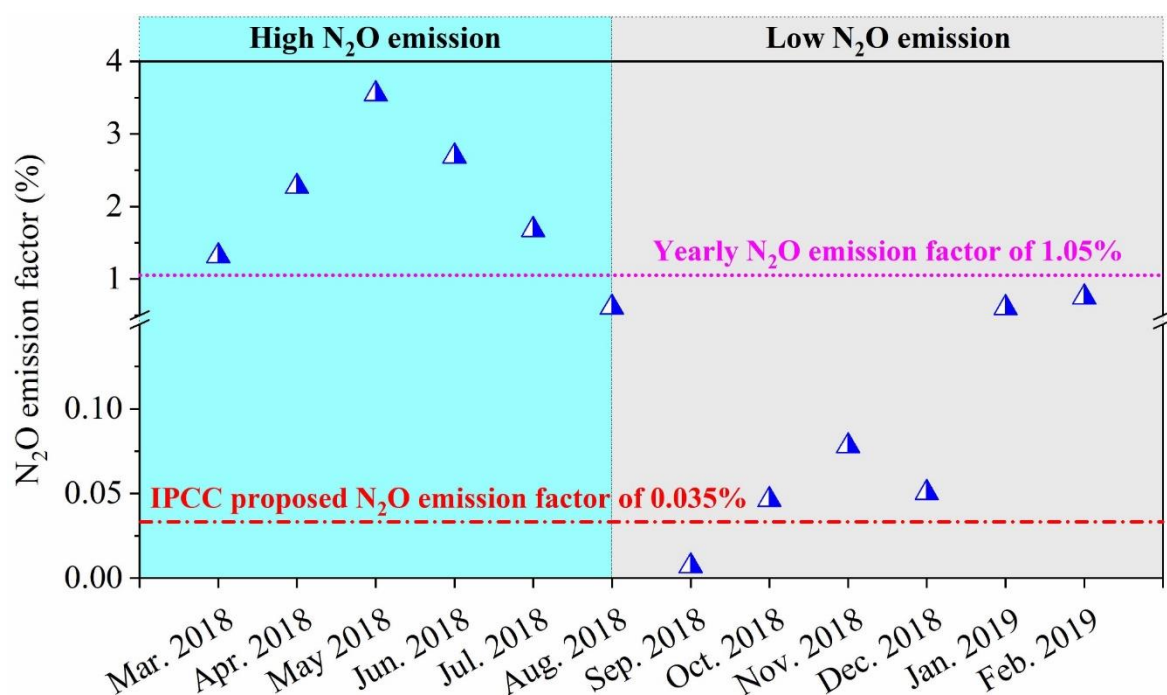


**Figure 6**. $N_2O$ emission factors of Reactor 3 over monitoring period and comparison with IPCC proposed level.

## 3.2. $N_2O$ Emission Characteristics and Correlations with Process Variables

In order to mitigate $N_2O$ emission effectively, control strategies are particularly needed in seasons with an increasing trend of water temperature (i.e., spring and summer), while their implementation in autumn and winter will further strengthen the abatement performance. As viable $N_2O$ control strategies need to deal with $N_2O$ emission dynamics under various process conditions, their development should be based on high-resolution analyses looking into the cyclic patterns associated with $N_2O$ emission in the reactors as well as the correlations between $N_2O$ emission and relevant process variables.

### 3.2.1. Recurring cyclic patterns in high N₂O emission seasons

**Fig. 7** delineates three types of recurring cyclic patterns in high $N_2O$ emission seasons, i.e., the sub-period with relatively high $N_2O$ emission identified in the previous section. Here a cycle was defined to consist of a preceding aerobic (aerated) phase and a following anoxic (non-aerated) phase, regulated by the STAR Control®.
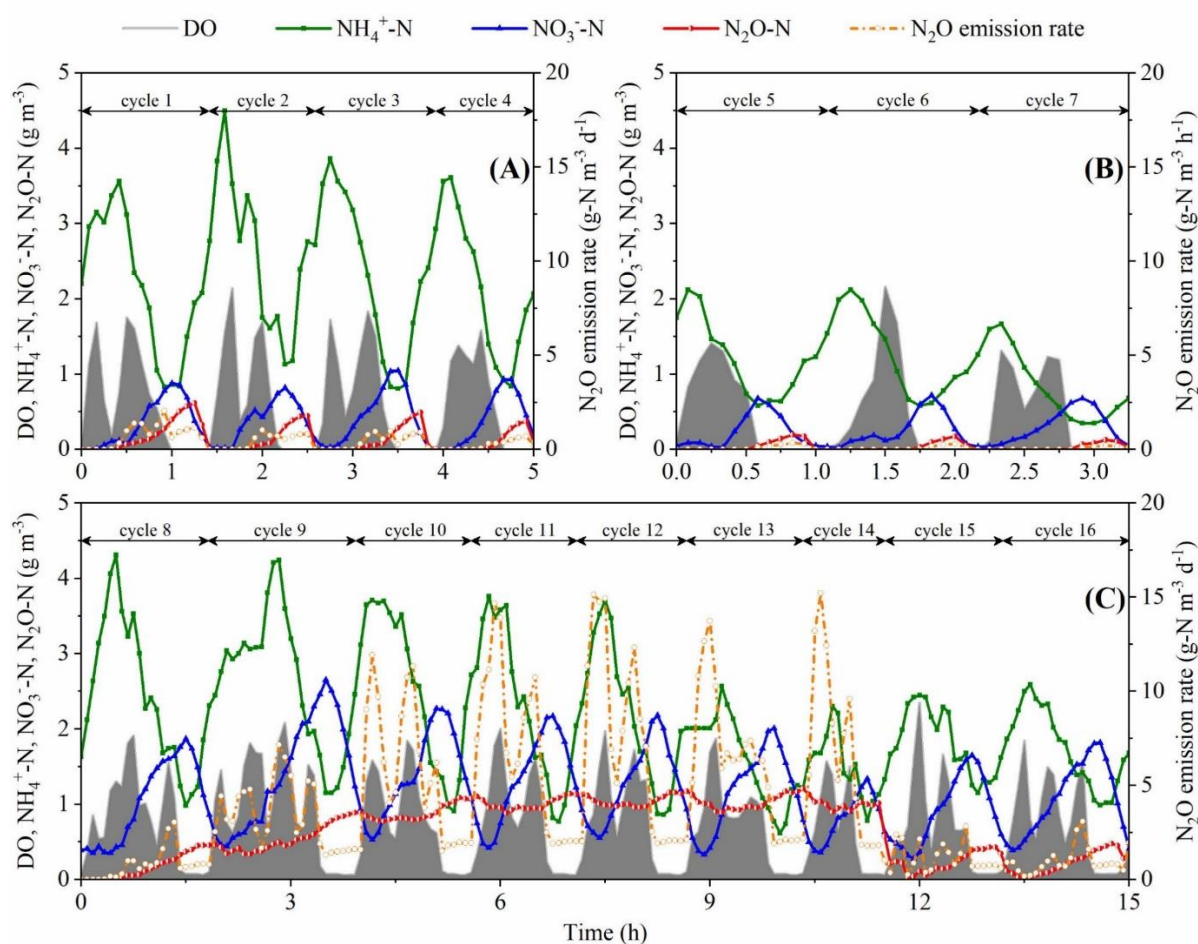


**Figure 7**. Three types of recurring cyclic patterns in seasons with relatively high $N_2O$ emission.

Cycles 1 to 4 in **Fig. 7A** represent the first type of recurring cyclic patterns. Upon the start of aeration in the aerobic phase, $NH_4^+$ firstly increased without significant formation of $NO_3^-$. This was due to the higher supply of $NH_4^+$ compared to its consumption through nitrification under limited DO conditions. $NO_2^-$, which was not specifically monitored at Avedøre WWTP, might to some extent accumulate. Therefore, the absence of $N_2O$ production therein might

indicate the insignificant role of the nitrifier denitrification pathway, which is typically triggered under low DO and/or high $NO_2^-$ conditions [12-16]. However, the potential contribution of the coexisting HB as the sole $N_2O$ scavenger in the reactors to $N_2O$ consumption could not be ruled out. Once DO reached a sufficiently high level, nitrification was enhanced. As a result, $NH_4^+$ started to decrease, accompanied by the formation of $NO_3^-$. The co-occurring $N_2O$ production under ample DO conditions might originate from the hydroxylamine pathway [14, 17, 18]. However, contrary to the reported simultaneous changes of nitrogenous compounds [14, 18], there existed an apparent lag phase between the emergence of $N_2O$ and the conversions of $NH_4^+$ and $NO_3^-$. This lag phase might be caused by the remaining heterotrophic $N_2O$ consumption under ample DO conditions, which was weakened with the formation of $NO_3^-$ due to the competition between different denitrification steps for electron donors [19, 20]. At the end of the aerobic phase, $NH_4^+$ arrived at the bottom level while $NO_3^-$ reached its peak. Once entering the anoxic phase, $NO_3^-$ decreased immediately due to denitrification, while $NH_4^+$ increased as a result of the consistent supply on top of the suspended nitrification process. Nevertheless, a different, non-monotonic behavior has been noticed for $N_2O$ production/emission. $N_2O$ firstly continued to increase for around 15 minutes, which clearly indicated the heterotrophic contribution to $N_2O$ production. When $NO_3^-$ decreased to a low level at the end of the anoxic phase, $N_2O$ started to be consumed and was depleted quickly. As nitrification was inactive in the anoxic phase, the observed trend between $N_2O$ and $NO_3^-$ was likely the result of the higher preference of HB for reducing $NO_3^-$ than $N_2O$ in the competition for limited electron donors [20, 21] or/and the presence of slowly biodegradable organics as electron donors which has been found to induce elevated $N_2O$ emission during denitrification [22, 23].

**Fig. 7B** shows the second type of recurring cyclic patterns. Compared to cycles 1 to 4 in **Fig. 7A**, the lowered $NH_4^+$ loadings in cycles 5 to 7 led to the lowered $N_2O$ production through the hydroxylamine pathway during nitrification. However, no $N_2O$ was actually detected in the aerobic phase. This phenomenon could only be caused by the heterotrophic $N_2O$ consumption as HB were the sole $N_2O$ scavenger in the reactors. Consequently, $N_2O$ production/emission only occurred in the anoxic phase. Despite the difference in magnitude, $NO_3^-$ and $N_2O$ had a correlation similar to the one observed in the first type of recurring cyclic patterns (i.e., **Fig. 7A**), further confirming the dual role of HB in $N_2O$ turnover in the anoxic phase.

The third type of recurring cyclic patterns which covered all the cycles with $N_2O$ emission peaks in high $N_2O$ emission seasons are exampled by cycles 8 to 16 in **Fig. 7C**. Cycle 8 was largely analogous to the first type of recurring cyclic patterns presented in **Fig. 7A**, where $N_2O$ was produced and emitted in both the aerobic and anoxic phases. The major difference lied in the disappearance of $N_2O$ consumption in the anoxic phase (i.e., incomplete denitrification), which might be explained by the relatively high $NO_3^-$ level at the end of the anoxic phase, thus placing the heterotrophic $N_2O$ consumption in a disadvantageous position in the competition for electron donors. This incomplete denitrification actually resulted from the inadequate length of anoxic phase determined by the STAR Control®. Once entering the following cycle (i.e., cycle 9), the $N_2O$ accumulated in the liquid phase got stripped immediately, thus generating high $N_2O$ emission. This phenomenon of significantly higher $N_2O$ emission from reactors with intermittent aeration or compartments switching between aerobic and anoxic phases has also been documented in other types of activated sludge systems [4, 24]. Despite the high $N_2O$ emission in the aerobic phase, the $N_2O$ level remained relatively stable, which might be due to i) the continuous $N_2O$ production during nitrification and ii) the depressed heterotrophic $N_2O$ consumption in the presence of the relatively high $NO_3^-$ level. On account of the sole heterotrophic $N_2O$ production contribution, the accumulation of $N_2O$ continued until the end of the anoxic phase. The accumulated $N_2O$ got carried over to the next cycle (i.e., cycle 10), thus causing significantly high $N_2O$ emission in the aerobic phase. This cyclic pattern persisted for several cycles until cycle 14, where the heterotrophic $N_2O$ consumption was observed in the anoxic phase (i.e., complete denitrification) due to the reduced $NO_3^-$ level compared to the preceding cycles. Consequently, $N_2O$ was removed from the liquid phase before entering the next cycle, which resembled the first type of recurring cyclic patterns (i.e., **Fig. 7A**) and therefore only incurred relatively low $N_2O$ emission (see cycles 15 and 16 in **Fig. 7C**).

### 3.2.2. Correlations between $N_2O$ emission and process variables

Pearson's partial correlation analysis was applied to explore the degree of association between $N_2O$ emission and each process variable, with the effects of other process variables removed. Following common practice, a PCC between 0 and 0.3 (0 and -0.3) was defined here to indicate a weak positive (negative) correlation, a PCC between 0.3 and 0.7 (-0.3 and -0.7) indicated a

moderate positive (negative) correlation, and a PCC between 0.7 and 1.0 (-0.7 and -1.0) indicated a strong positive (negative) correlation. The two sub-periods identified in **Fig. 5A** were analyzed separately to probe into the change in the dependency of $N_2O$ emission on relevant process variables. Considering their significant difference in operational conditions and control scheme, the aerobic and anoxic phases, each accounting for around 85% and 15% of $N_2O$ emission on both monthly and yearly scale, were also analyzed separately in the partial correlation analysis.
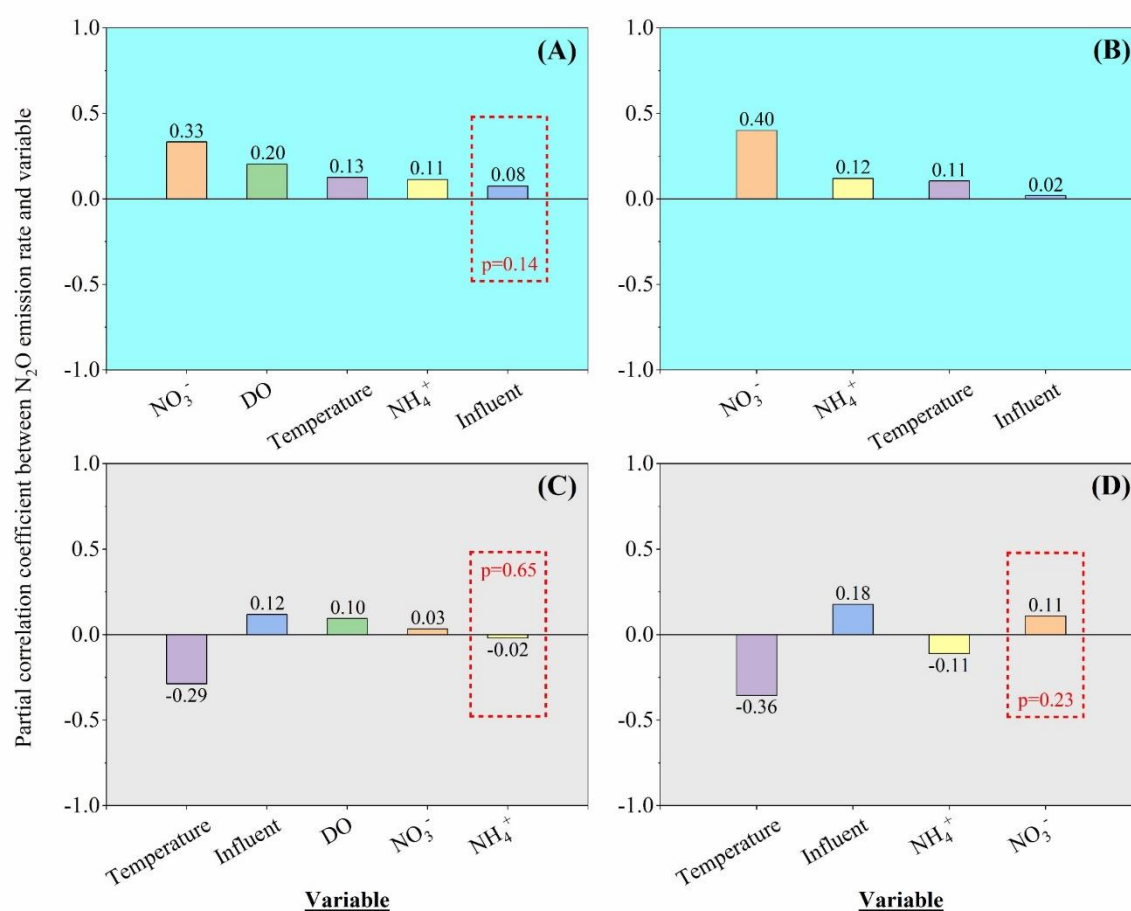


**Figure 8**. Pearson's partial correlation coefficients between monitored process variables and $N_2O$ emission rate in (**A** and **C**) aerobic and (**B** and **D**) anoxic phase of seasons with relatively (**A** and **B**) high and (**C** and **D**) low $N_2O$ emission (Highlighted box indicates partial correlation coefficient not significantly different from zero, i.e., p>0.05).

**Fig. 8A** illustrates the PCC between $N_2O$ emission rate and process variables (including influent flowrate, DO, $NH_4^+$, $NO_3^-$, and water temperature) in the aerobic phase of the sub-period with relatively high $N_2O$ emission. Among all the process variables studied, only $NO_3^-$ had a moderate positive correlation (PCC=0.33, p=0.00) with $N_2O$ emission rate, which might indicate the main contribution of the hydroxylamine pathway during nitrification to the $N_2O$ production/emission. This was also supported by the weak positive correlations of $N_2O$ emission rate with DO (PCC=0.20, p=0.00) and $NH_4^+$ (PCC=0.11, p=0.00), which have been shown to possess a positive impact on the hydroxylamine pathway [14, 17, 18]. Water temperature also had a weak positive correlation (PCC=0.13, p=0.00) with $N_2O$ emission rate, which might be due to the positive relationship between overall kinetics of nitrogen conversion processes and water temperature in the studied range (i.e., between 10 °C and 20 °C) and was consistent with Ahn et al.[5]. Influent flowrate was found to insignificantly correlate with $N_2O$ emission rate (PCC=0.08, p=0.14). As full nitrification was pursued at the studied WWTP through implementing high DO set-point (i.e., lowest DO set-point of 0.5 g m$^{-3}$ when $NH_4^+$ is 0 g-N m$^{-3}$) and existing criteria of aerobic phase based on the in-situ $NH_4^+$/$NO_3^-$ relationship in the STAR Control®, $NO_2^-$ wouldn't have a significant impact on $N_2O$ emission, although it has been found to highly correlate with $N_2O$ emission in other activated sludge systems [7, 25]. **Fig. 8B** exhibits the PCC between $N_2O$ emission rate and process variables (including influent flowrate, $NH_4^+$, $NO_3^-$, and water temperature) in the anoxic phase of the sub-period with relatively high $N_2O$ emission. Compared to the weakly correlated influent flowrate, $NH_4^+$, and water temperature, $NO_3^-$ had a moderate positive correlation (PCC=0.40, p=0.00) with $N_2O$ emission rate, supporting the hypothesis that incomplete denitrification (caused by the competition between heterotrophic $NO_3^-$ and $N_2O$ reduction for electron donors) contributed mainly to the $N_2O$ production/emission in the anoxic phase.

Distinct results were obtained in the counterpart analysis on the aerobic (**Fig. 8C**) and anoxic (**Fig. 8D**) phases of the sub-period with relatively low $N_2O$ emission. The first major difference lied in water temperature which appeared to have an around moderate negative correlation with $N_2O$ emission rate (i.e., PCC of -0.29 for the aerobic phase and -0.36 for the anoxic phase). The second major difference was associated with $NO_3^-$ which was found to be weakly correlated or uncorrelated with $N_2O$ emission rate. Although none of the studied process

variables in **Fig. 8** had a strong correlation with $N_2O$ emission rate (e.g., PCC>0.7), most of them were found to be significant factors (P value lower than 0.05). This indicates that $N_2O$ emission is a complex nonlinear phenomena affected by all key process variables. Given the significant discrepancy between **Figs. 8A-B** and **Figs. 8C-D,** there might be other process variables affecting $N_2O$ emissions which were not accounted for in this analysis. For example, the microbial community structure might shift significantly in response to the declining trend in water temperature but remain relatively stable when facing the increasing water temperature, thus leading to the opposite PCC between water temperature and $N_2O$ emission rate as well as the different significance of $NO_3^-$ in affecting $N_2O$ emission in **Figs. 8A-B** and **Figs. 8C-D**. Alternative and robust statistical analysis methods are needed to cross check the results of PCC.

## 3.3. Impact of Changed DO Set-Point on $N_2O$ Emission at Avedøre WWTP

As explained in **Section 2.3**, DO set-point in the STAR® control system of Avedøre WWTP was manipulated to test the main component of the fuzzy logical controller aiming to regulate the activities of AOB and NOB.
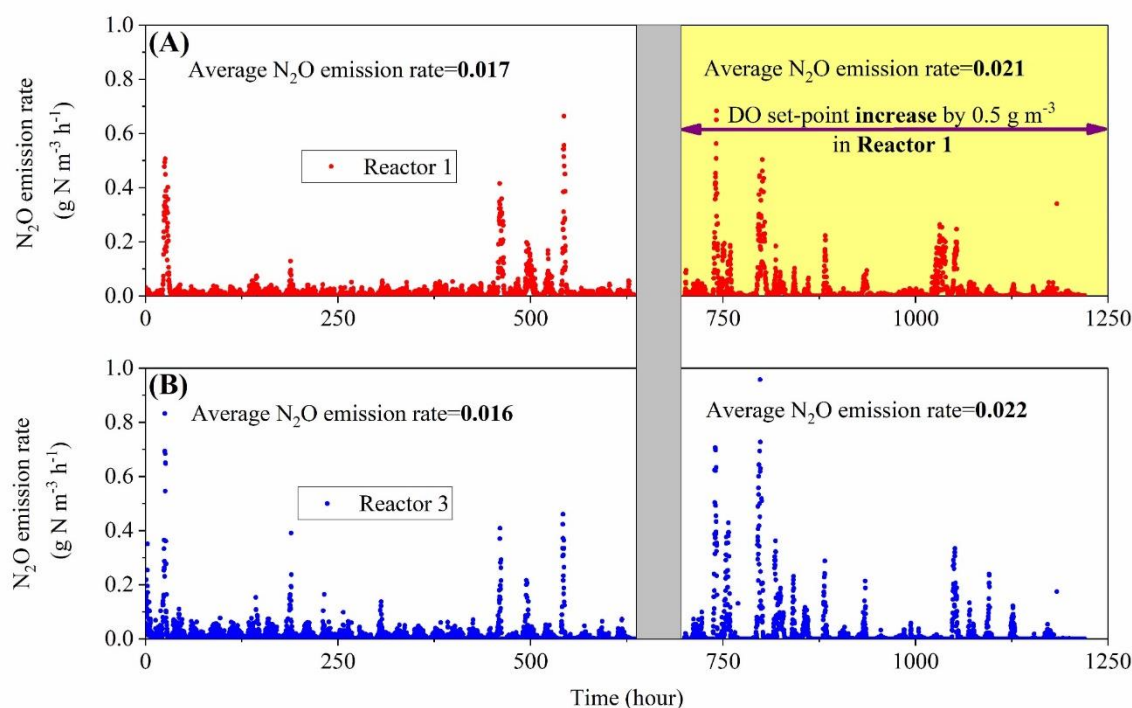


**Figure 9**. Comparison of $N_2O$ emission rate between (**A**) Reactor 1 with increased DO set-point and (**B**) Reactor 3 without increased DO set-point.

**Fig. 9** demonstrates the impact of increased DO set-point on $N_2O$ emission rate carried out in **August 2018**. As evidenced by the similar dynamic change and average level of the $N_2O$ emission rate in Reactor 1 and Reactor 3, the increased DO set-point didn't bring about significant changes to the $N_2O$ emission rate at Avedøre WWTP.

As illustrated in **Fig.10** which compares the $N_2O$ emission rate between reactors with and without decreased DO set-point carried out in **May 2019**, a decreased DO set-point in Reactor 3 led to $N_2O$ emission 60% lower than Reactor 1. After reverting the DO set-point in Reactor 3 back to the original level, the $N_2O$ emission rate in Reactor 3 was still lower than Reactor 1. However, the discrepancy was closing up, and the $N_2O$ emission rates in Reactor 1 and Reactor 3 might level up in ample time.
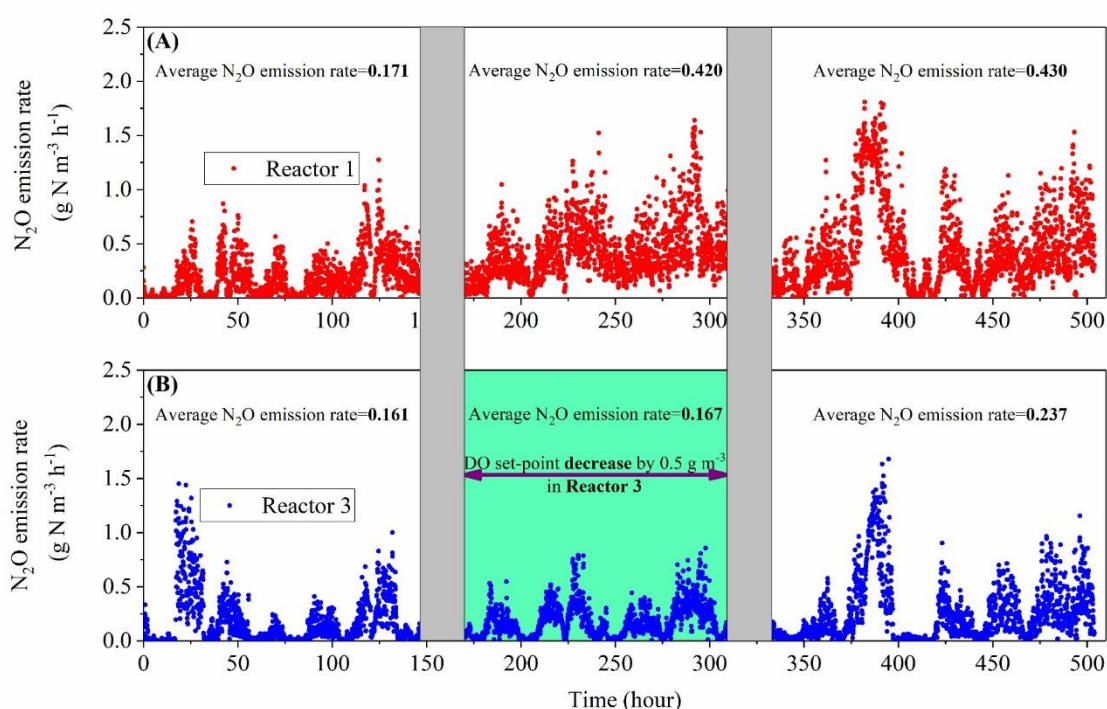


**Figure 10**. Comparison of $N_2O$ emission rate between (**A**) Reactor 1 without decreased DO set-point and (**B**) Reactor 3 with decreased DO set-point.

## 3.4. Implications for $N_2O$ Emission Control and Future Work

As unveiled in **Section 3.2**, HB had a dual role in the anoxic phase and could be responsible for both net $N_2O$ production and consumption, which tended to take place in sequence probably

resulting from the competition between different denitrification steps for electron donors. Therefore, in order to avoid the accumulation of $N_2O$ as a result of incomplete denitrification which would be carried over to the following cycles and therefore subject to high emission, sufficient usage of the heterotrophic $N_2O$ consuming capability of the anoxic phase (i.e., complete denitrification) should be guaranteed through relevant control strategy such as extending the length of anoxic phase or adding external carbon source. Practically, the peak $NH_4^+$ level and the ending $NO_3^-$ level in the aerobic phase of a certain cycle could be used as indicators of the need for relevant control strategy in the following anoxic phase. As shown in **Fig. 11**, when the peak $NH_4^+$ level and the ending $NO_3^-$ level in the aerobic phase nearly double compared to the conventional levels, it would be highly likely that $N_2O$ would accumulate at the end of the cycle and then get carrier over to the subsequent cycle, thus triggering high $N_2O$ emission. In this case, the aforementioned control strategy should be executed timely to prevent $N_2O$ emission peaks (i.e., significantly high $N_2O$ emission in the aerobic phase of cycles 9 to 14 in **Fig. 7C**). In fact, this finding regarding the important role of denitrification in mitigating $N_2O$ emission should be applicable to other activated sludge reactors with intermittent aeration or compartments switching between aerobic and anoxic phases. In Europe, according to relevant statistics, there are over 80 WWTPs that are using the STAR Control® as their control solution. For these plants, when needed, the current control system could be readily modified to reduce $N_2O$ emission through wisely controlling the anoxic phase.

Comparatively, control over the aerobic phase should be based more on the fact that the hydroxylamine pathway during nitrification dominated the $N_2O$ production. Therefore, a decreased DO set-point might help reduce the $N_2O$ production through the hydroxylamine pathway, which has been verified in this project though the decreased DO set-point test carried out at Avedøre WWTP (see **Fig. 10**). An accompanying benefit of applying a decreased DO set-point is the lower energy input in terms of aeration (e.g., 15% aeration reduction for the decreased DO set-point test in **Fig. 10**). Moreover, as heterotrophic $N_2O$ consumption mediated by the coexisting HB might also play a role in the aerobic phase, addition of external carbon source or fractional diversion of influent into the aerobic phase might serve as another potential approach. However, in this case, a majority of externally added carbon source might be oxidized

directly (i.e., without providing effective electron donors for simultaneous denitrification in the aerobic phase).
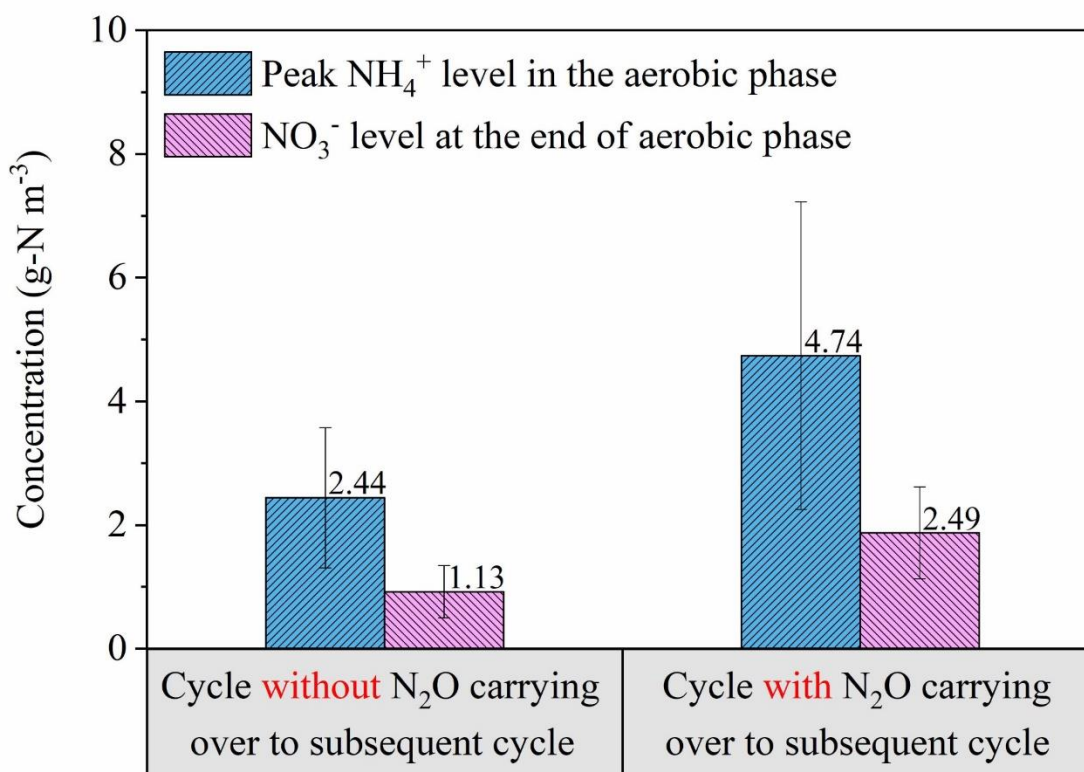


**Figure 11**. Comparison of peak $NH_4^+$ level in aerobic phase and $NO_3^-$ level at the end of aerobic phase between cycles without and with $N_2O$ carrying over to subsequent cycle in peak $N_2O$ emission month.

The fact that the hydroxylamine pathway by AOB and the heterotrophic activity were mainly responsible for the $N_2O$ production/emission at Avedøre WWTP implies that the developed fuzzy logic controller [8] might not be sufficient in reducing $N_2O$ emission as it is based mainly on the nitrifier denitrification pathway by AOB. While the results confirmed/verified the basic assumption of the fuzzy logic controller that regulating DO set-point helps lower $N_2O$ emission in the aerated phase, the fuzzy logic controller alone is not sufficient to address the $N_2O$ contribution from the anoxic phase due to the denitrification process. In this case, the $N_2O$ control strategies proposed in this project are of significant value. However, it should be acknowledged that the proposed control strategy over the anoxic phase

needs to be validated through some prospective short-term full-scale experiments. Additionally, although Foley et al.[10] claimed that the concentrations of nitrogenous compounds could be assumed to approach perfectly mixed conditions in a Carrousel compartment, the real uniformity of each process variable is barely possible to achieve at full-scale WWTPs. Potential spatial heterogeneity could be checked by placing a second set of measuring sensors in the compartment. However, the fact that the existing sensors are installed around the same place ensures the comparability between process variables, laying the solid foundation for the analyses we have done. Besides the one-year data presented, the availability of more data is highly desired to clarify whether $N_2O$ emission would differ from year to year. The hypotheses regarding the $N_2O$ production pathways could be proved/tested with the availability of on-line $NO_2^-$ and COD measurements as well as the help of in-situ isotope tracing techniques [26] and sophisticated mathematical modelling, which are the focus of future work.

# 4. CONCLUSIONS

- We have successfully performed a long-term (12-month) monitoring campaign of $N_2O$ emission at Avedøre WWTP. Results show that relatively low $N_2O$ emission took place in seasons with a decreasing trend of water temperature, while relatively high $N_2O$ emission occurred in seasons with an increasing trend of water temperature, when control strategies should be implemented in particular for mitigating $N_2O$ emission.

- Aerobic phase contributed to $N_2O$ production/emission mainly through the hydroxylamine pathway by AOB, while heterotrophic denitrification had a dual role in the anoxic phase and could be responsible for both net $N_2O$ production and consumption. Full denitrification in the anoxic phase should be ensured so that the accumulated $N_2O$ wouldn't be carried over to the following cycle where significantly high $N_2O$ emission would occur.

- With the peak $NH_4^+$ level and the ending $NO_3^-$ level in the preceding aerobic phase as indicators, potential control over the anoxic phase could include extending the length of anoxic phase or adding external carbon source as a means to regulate $N_2O$ accumulation in the anoxic phase.

- Control over the aerobic phase could include introducing a decreased DO set-point in the control system, which would curb the $N_2O$ production via the hydroxylamine pathway by

AOB and has been verified through full-scale testing at Avedøre WWTP. This verified the basic concept of the fuzzy logic controller about regulating the DO set-point to maintain low $N_2O$ emission from the aerobic phase.

- A significant contribution to $N_2O$ emission was also contributed by the denitrification process in the anoxic phase. This shows that the fuzzy logic controller alone is not sufficient in reducing $N_2O$ emission from WWTPs with plant configuration and control solution similar to Avedøre WWTP. Proper extension/modification of the developed fuzzy logic controller is needed to account for the denitrification process.

# 5. ACKNOWLEDGEMENT

# 6. REFERENCES

1. IPCC *Climate Change 2014: Synthesis Report. Contribution of Working Groups I, II and III to the Fifth Assessment Report of the Intergovernmental Panel on Climate Change*; IPCC, Geneva, Switzerland, 2014; p 151.

2. Hanaki, K.; Hong, Z.; Matsuo, T. Production of Nitrous Oxide Gas during Denitrification of Wastewater. *Water Sci. Technol.* **1992,** *26*, (5-6), 1027-1036.

3. Czepiel, P.; Crill, P.; Harriss, R. Nitrous Oxide Emissions from Municipal Wastewater Treatment. *Environ. Sci. Technol.* **1995,** *29*, (9), 2352-2356.

4. Aboobakar, A.; Cartmell, E.; Stephenson, T.; Jones, M.; Vale, P.; Dotro, G. Nitrous oxide emissions and dissolved oxygen profiling in a full-scale nitrifying activated sludge treatment plant. *Water Res.* **2013,** *47*, (2), 524-534.

5. Ahn, J. H.; Kim, S.; Park, H.; Rahm, B.; Pagilla, K.; Chandran, K. N2O Emissions from Activated Sludge Processes, 2008−2009: Results of a National Monitoring Survey in the United States. *Environmental Science & Technology* **2010,** *44*, (12), 4505-4511.

6. Yoshida, H.; Mønster, J.; Scheutz, C. Plant-integrated measurement of greenhouse gas emissions from a municipal wastewater treatment plant. *Water Research* **2014,** *61*, 108-118.

7. Daelman, M. R. J.; van Voorthuizen, E. M.; van Dongen, U. G. J. M.; Volcke, E. I. P.; van Loosdrecht, M. C. M. Seasonal and diurnal variability of N2O emissions from a full-scale municipal wastewater treatment plant. *Science of The Total Environment* **2015,** *536*, 1-11.

8. Boiocchi, R.; Gernaey, K. V.; Sin, G. A novel fuzzy-logic control strategy minimizing N2O emissions. *Water Res.* **2017,** *123*, 479-494.

9. Schulthess, R. V.; Gujer, W. Release of nitrous oxide (N2O) from denitrifying activated sludge: Verification and application of a mathematical model. *Water Res.* **1996,** *30*, (3), 521-530.

10. Foley, J.; de Haas, D.; Yuan, Z.; Lant, P. Nitrous oxide generation in full-scale biological nutrient removal wastewater treatment plants. *Water Res.* **2010,** *44*, (3), 831-844.

11. Marques, R.; Rodriguez-Caballero, A.; Oehmen, A.; Pijuan, M. Assessment of online monitoring strategies for measuring N2O emissions from full-scale wastewater treatment systems. *Water Research* **2016,** *99*, 171-179.

12. Peng, L.; Ni, B.-J.; Ye, L.; Yuan, Z. The combined effect of dissolved oxygen and nitrite on N2O production by ammonia oxidizing bacteria in an enriched nitrifying sludge. *Water Res.* **2015,** *73*, (0), 29-36.

13. Kampschreur, M. J.; Tan, N. C. G.; Kleerebezem, R.; Picioreanu, C.; Jetten, M. S. M.; Loosdrecht, M. C. M. Effect of dynamic process conditions on nitrogen oxides emission from a nitrifying culture. *Environ. Sci. Technol.* **2008,** *42*, (2), 429-435.

14. Peng, L.; Ni, B.-J.; Erler, D.; Ye, L.; Yuan, Z. The effect of dissolved oxygen on N2O production by ammonia-oxidizing bacteria in an enriched nitrifying sludge. *Water Res.* **2014**, (0).

15. Wunderlin, P.; Mohn, J.; Joss, A.; Emmenegger, L.; Siegrist, H. Mechanisms of N2O production in biological wastewater treatment under nitrifying and denitrifying conditions. *Water Res.* **2012,** *46*, (4), 1027-1037.

16. Rassamee, V.; Sattayatewa, C.; Pagilla, K.; Chandran, K. Effect of Oxic and Anoxic Conditions on Nitrous Oxide Emissions from Nitrification and Denitrification Processes. *Biotechnol. Bioeng.* **2011,** *108*, (9), 2036-2045.

17. Chandran, K.; Stein, L. Y.; Klotz, M. G.; van Loosdrecht, M. C. M. Nitrous oxide production by lithotrophic ammonia-oxidizing bacteria and implications for engineered nitrogen-removal systems. *Biochem. Soc. Trans.* **2011,** *39*, 1832-1837.

18. Chen, X.; Yuan, Z.; Ni, B.-J. Nitrite accumulation inside sludge flocs significantly influencing nitrous oxide production by ammonium-oxidizing bacteria. *Water Res.* **2018,** *143*, 99-108.

19. Chen, X.; Ni, B.-J.; Sin, G. Nitrous Oxide Production in Autotrophic Nitrogen Removal Granular Sludge: A Modeling Study. *Biotechnol. Bioeng.* **2019,** *0*, (ja).

20. Pan, Y. T.; Ni, B. J.; Bond, P. L.; Ye, L.; Yuan, Z. G. Electron competition among nitrogen oxides reduction during methanol-utilizing denitrification in wastewater treatment. *Water Res.* **2013,** *47*, (10), 3273-3281.

21. Ni, B. J.; Yuan, Z. G. Recent advances in mathematical modeling of nitrous oxides emissions from wastewater treatment processes. *Water Res.* **2015,** *87*, 336-346.

22. Schalk-Otte, S.; Seviour, R. J.; Kuenen, J. G.; Jetten, M. S. M. Nitrous oxide (N2O) production by Alcaligenes faecalis during feast and famine regimes. *Water Res.* **2000,** *34*, (7), 2080-2088.

23. Massara, T. M.; Malamis, S.; Guisasola, A.; Baeza, J. A.; Noutsopoulos, C.; Katsou, E. A review on nitrous oxide (N2O) emissions during biological nutrient removal from municipal wastewater and sludge reject water. *Sci. Total Environ.* **2017,** *596*, 106-123.

24. Yang, Q.; Liu, X.; Peng, C.; Wang, S.; Sun, H.; Peng, Y. N2O Production during Nitrogen Removal via Nitrite from Domestic Wastewater: Main Sources and Control Method. *Environ. Sci. Technol.* **2009,** *43*, (24), 9400-9406.

25. Vasilaki, V.; Volcke, E. I. P.; Nandi, A. K.; van Loosdrecht, M. C. M.; Katsou, E. Relating N2O emissions during biological nitrogen removal with operating conditions using multivariate statistical techniques. *Water Research* **2018,** *140*, 387-402.

26. Wunderlin, P.; Lehmann, M. F.; Siegrist, H.; Tuzson, B.; Joss, A.; Emmenegger, L.; Mohn, J. Isotope Signatures of N2O in a Mixed Microbial Population System: Constraints on N2O Producing Pathways in Wastewater Treatment. *Environ. Sci. Technol.* **2013,** *47*, (3), 1339-1348.